

EFFICIENT FUZZY LOGIC SPEED CONTROL FOR VARIOUS TYPES OF DC MOTORS SUPPLIED BY PHOTOVOLTAIC SYSTEM UNDER MAXIMUM POWER POINT TRACKING

Ali Mohamed Yousef Ali¹ and Ahmed Said Oshaba²

¹Electric Engineering Department, Faculty of Engineering, Assiut University, Egypt , Email: drali_yousef@yahoo.com

²Electronics Research Institute, Power Electronics and Energy Conversions NRC Bldg., El-Tahrir St., Dokki, 12311-Giza, Egypt, Email : oshaba68@hotmail.com

(Received June 20, 2012 Accepted July 5, 2012)

This paper presents an efficient fuzzy logic speed controller (EFLSC) for various types of DC motors (permanent magnet DC motor and series DC motor). These DC motors are fed by the maximum power point tracking (MPPT) for photovoltaic (PV) arrays by using DC/DC converter between the PV array and DC motors. The speed controller explores the idea of the efficient fuzzy logic controller in a classical form. This controller combines the advantages of the classical controller and the intelligent properties of the fuzzy logic controller. The controller constants can be easily calculated based on the mechanical equation of the DC motors and a defined speed performance. The mechanical equations for the permanent magnet DC motor and series DC motor are represented by a first and second order differential equations respectively. This is used to change the duty cycle of the converter and thereby, the voltage fed to the DC motor to regulate its speed. The performance of these motors for load variation and speed change has been reported. The proposed controller shows that the EFLSC based DC-DC drive can have better control performance. In addition, this paper presents a proportional, integral and derivative (PID) controller method for maximum power point tracking of photovoltaic systems under different atmospheric conditions and variable output loads.

Keywords: Photovoltaic system, Solar cells, MPPT, DC-Series Motor, permanent magnet DC motor, EFLSC intelligent speed controller.

1. INTRODUCTION

In recent years, the fuzzy logic/set theory has been utilized for various control applications including motor control. The fuzzy logic has made the control of complex non linear systems with unknown or un-modeled dynamics as simple as possible [1]. The application of DC motor as suitable drive system in industrial environment has increased due to its high performance and high starting torque. There have been several conventional control techniques in DC motor drives are [2] and [3]. Hence the tuning and optimization of these controllers is a challenging and difficult task, particularly, under varying load conditions, parameter changes, abnormal modes of operation.

The sun is a great source of energy. Most of the energy is in the form of light and heat, which can be collected and used for generating electricity, as well as for heating, cooling and lighting building. Photovoltaic cells are large-area semiconductors that convert sunlight directly into electricity. Photovoltaic systems become a very attractive solution due to the energy crisis and environment issues such as pollution and global warming effect. Recently, photovoltaic systems have seen use in even more remote applications as cost comes down such as wireless highway call boxes, and stand alone power generation units. Photovoltaic generation is gaining increased importance as a renewable source due to its advantages [1,2], such as the absence of fuel cost, little maintenance, no noise, and wear due to the absence of moving parts, etc.

The actual energy conversion efficiency of PV module is rather low and is affected by the weather conditions and output load. So, to overcome these problems and to get the maximum possible efficiency, the design of all the elements of the PV system has to be optimized. The PV array has a highly nonlinear current-voltage characteristics varying with solar illumination and operating temperature [3,4], that substantially affects the array power outputs. At particular solar illumination, there is unique operating point of PV array at which it's power output is maximum. Therefore, for maximum power generation and extraction efficiency, it is necessary to match the PV generator to the load such that the equilibrium operating point coincides with the maximum power point of the PV array. The maximum power point tracking (MPPT) control is therefore critical for the success of the PV system [5 to 10].

The proposed system utilizes the MPPT technique to feed the overall speed control system for different types of DC motor. The EFLSC controller is used for speed control. This speed controller is used to adjust the duty cycle of the PWM switching signal of another step-down and step-up chopper (buck-boost, and converters) DC to DC converter. The drive system has the advantages of precise, fast, effective speed reference tracking without any overshoot (critical damping) and minimal steady state error. The fuzzy logic based speed command profile is followed even under load torque disturbances.

2. PROPOSED SYSTEM

Figures 1 and 2 show the block diagram and the Matlab/Simulink of the proposed system. The system consists of PV system, MPPT controller, DC-DC converter for MPPT, speed controller and DC-DC converter to drive the DC motor. In the MPPT control loop (by using PID controller), the resistance load error signal is obtained by comparing the reference load resistance and its actual values. But in the speed control loop (by using fuzzy logic controller), the speed error signal is obtained by comparing between the reference speed and the actual motor speed. From the present and previous errors the change in error is calculated. The following illustrates the overall system construction.

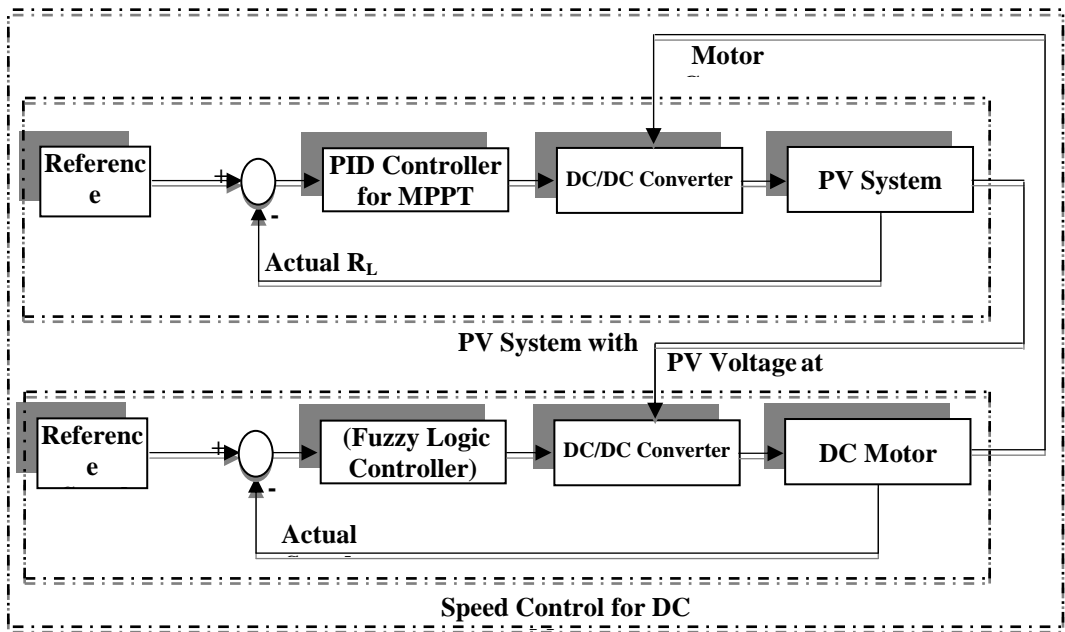


Fig. 1: Overall block diagram of DC control system supplied by PV system at MPPT.

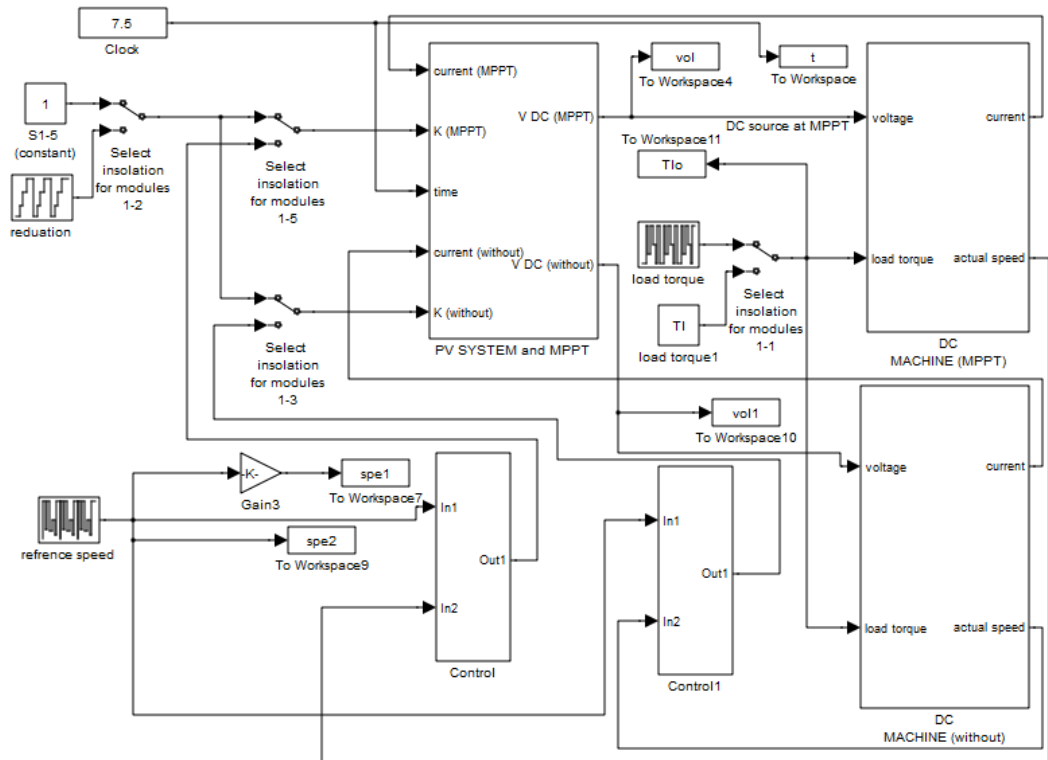


Fig. 2: Overall Matlab system for DC control system supplied by PV system at MPPT

3. SOLAR CELL MODELING

Solar cell mathematical modeling is an important step in the analysis and design of PV control systems to obtain the MPPT. The PV mathematical model can be obtained by following [5-10]:

$$I_c = I_{ph} - I_o \left\{ e^{\left[\frac{q}{AKT}(V_c + I_c R_s) \right]} - 1 \right\} \quad (1)$$

$$V_c = \frac{AkT}{q} \ln \left(\frac{I_{ph} + I_o - I_c}{I_o} \right) - I_c R_s \quad (2)$$

$$I = I_{ph} - I_o \left\{ e^{\left[\frac{q}{n_s AKT}(V + n_s I R_s) \right]} - 1 \right\} \quad (3)$$

$$V = \frac{n_s AkT}{q} \ln \left(\frac{I_{ph} + I_o - I}{I_o} \right) - n_s I R_s \quad (4)$$

where;

$$I_{ph} = \frac{G}{1000} [I_{sc} + k_i (T - T_r)]$$

$$I_o = I_{or} \left(\frac{T}{T_r} \right)^3 e^{\left[\frac{qE_g}{AK} \left(\frac{1}{T_r} - \frac{1}{T} \right) \right]}$$

The module output power can be determined simply from:

$$P = VI \quad (5)$$

where,

I_o = The reverse saturation current,

I_{ph} = The light generation current,

I = The photoelectric output current,

I_{sc} = The short circuit current,

A = The ideality factor,

V = The photoelectric voltage,

R_s = The module series resistance,

n_s = The number of series connected solar cells

k = The Boltzmann's constant,

q = The magnitude of the electron charge,

T = The absolute temperature,

G = The isolation value.

4. MAXIMUM POWER POINT TRACKING

As the power supplied by the solar array depends on the illumination, temperature and PV array power (voltage and current), an important consideration in the model for efficient solar array systems is to track the maximum power point correctly [10,11]. The purpose of the MPPT is to move the array operating voltage close to the MPP under changing atmospheric conditions and load. So far, three methods were often used to achieve the MPPT, these are; perturbation and observation method [12,13], incremental conductance method [14,15] and intelligent method [16,17]. The perturbation and observation method has been widely used due to its simple feedback structure and fewer measured parameters [12,13]. The peak power tracker operates by periodically incrementing or decrementing the solar array voltage. If a given perturbation leads to an increase (decrease) in array power, the subsequent perturbation is made in the same (opposite) direction. In this manner, the peak power tracker continuously hunts or seeks the peak power condition. Although this algorithm benefits from simplicity, it lacks the speed and adaptability necessary for tracking fast changing atmospheric conditions. The control system oscillates around the MPP forward and backward, and even tracking in a wrong way under rapidly changing atmospheric conditions. This method ignores the atmospheric conditions changing. The incremented conductance method [14,15] is based on the principle that the maximum power point ($dP/dV=0$), and since $P=V*I$, it yields $dV/dI = V/I$. A PID controller is used to regulate the PWM control signal of the DC/DC converter until the condition $(dV/dI)+(1/V) = 0$ is satisfied. Although, the incremental conductance method offers good performance under rapidly changing atmospheric conditions, it lacks from the circuit complexity, four sensor devices require more conversion time which result in a large amount of power loss and results in a higher system cost [5-10].

5. DC-DC CONVERTER

The choice of what DC-DC converter technology to use, can have a significant impact on both efficiency and effectiveness. Many converters have been used and tested; buck converter is a step down converter, while Boost converter is a step up converter [18]. In this research, a hybrid (buck and boost) DC/DC converter is used. Also, two DC-DC converters, the first of which is for MPPT and the second is for coupling between PV complete system and DC motor are given in Fig. 3. Such a technique is useful in PV systems because it allows the converter to extract the full available power from a module regardless of the illumination current or battery charge state. The equations for this converter type in continuous conduction mode are:

$$V_B = \frac{-K}{1-K} V_{ph} \quad (6)$$

And the corresponding current;

$$i_B = \frac{K-1}{K} i_{ph} \quad (7)$$

where K is the duty cycle of the PWM switching signal [5-10].

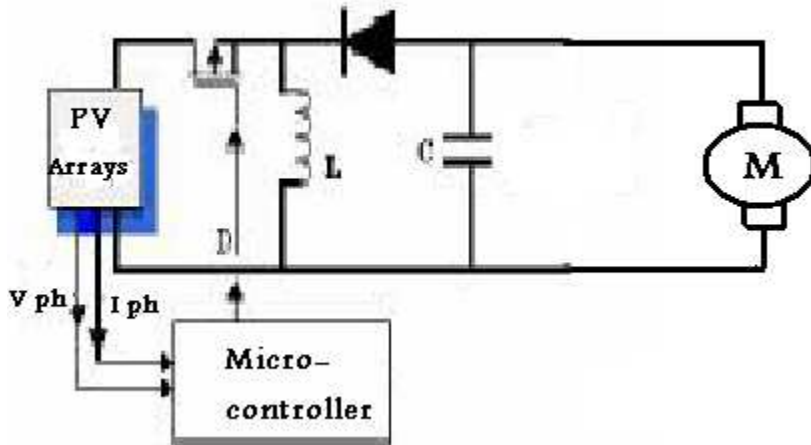


Fig. 3: DC-DC converter equivalent circuit.

6. PID- MPPT CONTROLLER

Proportional-integral-differential (PID) controller has being widely used in drive system. More than 90% of industrial controllers are implemented based on PID algorithms [3,4] and [19-23].The use of proportional-integral and derivative action (PID) together is very common.

The Proportion: can increase the response output of the controller and the control accuracy of the system.

The Integration: is used to eliminate the steady-state error of the system (one reason is that the integral action gives the system the capability to adjust itself to new load Conditions that require changes in the zero error control output (resetting action).

The Differentiation: can improve the dynamic performance of the system. It can inhibit and predict the change of the error in any direction.

The transfer function of the PID controller is:

$$G_s(s) = K_p + K_I / s + K_D \frac{d}{dt} \quad (8)$$

If $e(t)$ is the input to the **PID** controller, the output CPID from the controller is given by:

$$CPID = K_p e(t) + K_I \int e(t)dt + K_D \frac{de(t)}{dt} \quad (9)$$

Thus at any instant of time the controller output is composed of two terms. One term is due to the accumulated area of error versus time, and the other is due to the present extent of the error [5-10].

7. EFFICIENT FUZZY LOGIC SPEED CONTROLLER (EFLSC) OPERATION

The EFLSC can be regarded as a set of heuristic decision rules that include the experience of a human operator. The fuzzy controller relates significant and observable variables to the control actions, and consists of a fuzzy relationship or algorithm. The input error time sequences; error and change in error are converted to fuzzy variables. These variables are evaluated by the control rules using the compositional rule of inference, and approximately computed control action is then reconverted to the crisp value required to regulate the process. So the essential elements in designing fuzzy controller include [11-18]:

- 1- Defining input and output variables.
- 2- Converting the input variables to fuzzy sets.
- 3- Determining the fuzzy control rules.
- 4- Reconverting the fuzzy control actions into crisp control actions.

In case of speed control, the speed error signal $e(k)$ and its rate of change $de(k)$ are selected as inputs to fuzzy logic controller. These are normalized into a common universe of discourse and their linguistic fuzzy subsets along with their membership grades defined using the functions. The fuzzy membership grades of the control input change in the fuzzy subsets are obtained based on the rules given by table 1. Then this normalized value of control input change is reconverted back to its actual level.

Table 1: Fuzzy Control Rule Decision.

De(k) e(k)	NB	NM	NS	ZE	PS	PM	PB
NB	PB	PB	PB	PB	PM	PS	ZE
NM	PB	PB	PB	PM	PS	ZE	NS
NS	PB	PB	PM	PS	ZE	NS	NM
ZE	PB	PM	PM	ZE	NS	NM	NB
PS	PM	PS	ZE	NS	NM	NB	NB
PM	PS	ZE	NS	NM	NB	NB	NB
PB	ZE	NS	NM	NB	NB	NB	NB

7.1. The Proposed Speed Controller Design Based on EFLSC

As an FL controller on its own is a PD controller equivalent [12], output of the speed FL controller is integrated in order to yield PI like behavior. Based on this fact, the following equation is suggested to represent the FL controller output in a classical form.

The following equation is suggested to represent the FL controller output in a classical form as follows:

The controller output is equal to the integration of :

$$[k_1(e(k) + k_2\Delta e(k))] \tag{10}$$

where k_1 and k_2 are scaling factors.

$$e(k) = \omega_m^* - \omega_m \quad (11)$$

$$\Delta e(k) = (\omega_m^* - \omega_m) - (\omega_{mo}^* - \omega_{mo}) \quad (12)$$

If ω_m^* is constant then:

$$de(k) = -(\omega_m - \omega_{mo}) \quad (13)$$

Hence, the control output become as:

$$[k_1[(\omega_m^* - \omega_m) - k_2(\omega_m - \omega_{mo})]] \quad (14)$$

7.2. The Controller Model

The EFLSC output equation can be represented in s-domain using MATLAB/SIMULINK program as shown in Fig.4.

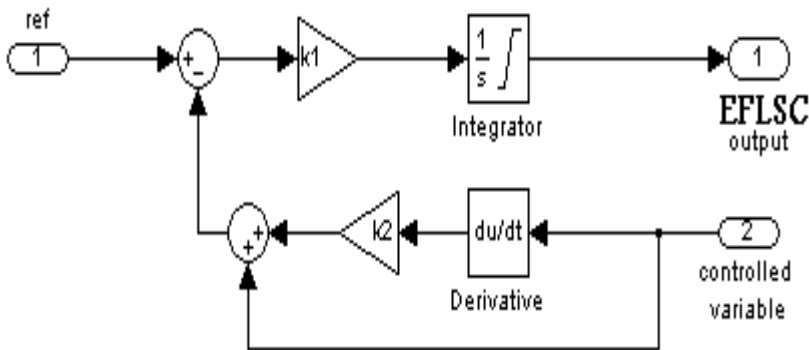


Fig. 4: EFLSC model in s-domain.

7.3. Determination of the EFLSC Parameters

To get the EFLSC parameters, the following equation is used to describe the motor operation:

$$T_e(t) = J \frac{d\omega_m(t)}{dt} + B\omega_m + T_L(t) \quad (15)$$

Simulating this equation with the EFLSC in s-domain, as shown in Fig. 5, reveals that the characteristics equation is given by (B is set to zero):

$$Js^2 + k_1k_2s + k_1 = 0 \quad (16)$$

and for a certain damped response of a reference speed step change, the following equation is valid:

$$k_2 = 2\sqrt{\frac{J\eta}{k_1}} \tag{17}$$

where η is the damping ratio.

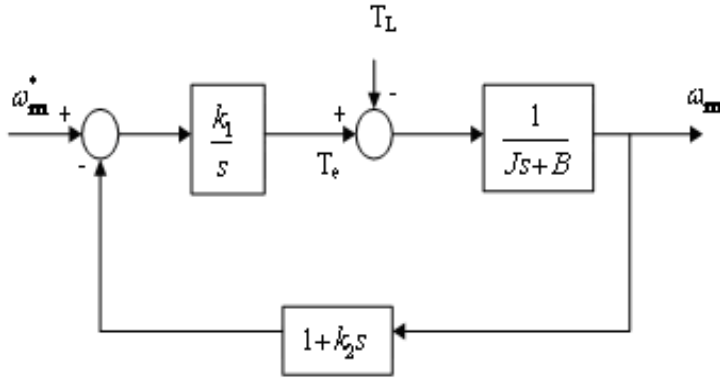


Fig. 5: Relation between reference and motor speed.

The relation between the motor speed and load torque, as shown in Fig. 6, can be obtained as follows:

$$\omega_m(s) = \frac{1}{\frac{k_1 * k_2}{J} s + 1} T_L(s) \tag{18}$$

For a step change of load torque the motor speed can be calculated as:

$$\omega_m(s) = \frac{1}{\left(\frac{J}{k_1 * k_2} s + 1\right)} \frac{T_L(s)}{(s)} \tag{19}$$

This represents a first order equation with a gain equals to:

$$M_{dip} = \frac{T_L}{k_1 * k_2} \tag{20}$$

This represents the maximum dip in motor speed at a load torque change from no load to full load. During transient in this case, the controller tries to reject this disturbance. Based on equations (18) and (20) the EFLSC parameters can be calculated to provide a motor speed with a certain damped response and a full load torque rejection with a predefined maximum dip. In equation (20) as $(k_1 * k_2)$ increases, the load torque disturbance rejection is faster and its maximum dip is smaller.

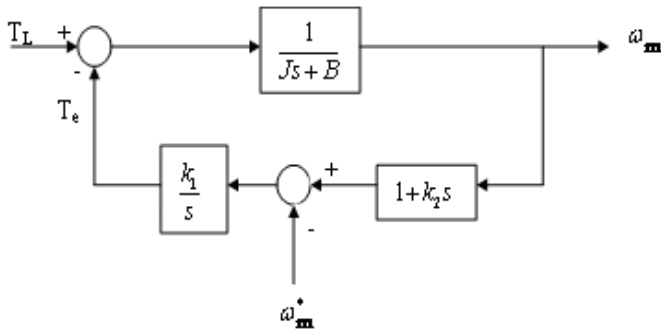


Figure 6 : Relation between load torque and motor speed.

8. DC SERIES MOTOR

8.1. DC Series Motor Construction

The field may be connected in series with the armature, resulting in a series DC machine. In the series machine, increase in load is accompanied by increases in the armature current and mmf and the stator field flux (provided the iron is not completely saturated). Because flux increases with load, speed must drop in order to maintain the balance between impressed voltage and counter emf. Moreover, the increase in armature current caused by increased torque is smaller than in the shunt machine because of the increased flux. The series machine is therefore a varying-speed machine with a markedly drooping speed-torque characteristic. For applications requiring heavy torque overloads, this characteristic is particularly advantageous because the corresponding power overloads are held to more reasonable values by the associated speed drops. Very favorable starting characteristics also result from the increase in flux with increased armature current [24-25].

The proposed system can be simulated with proper mathematic modeling. The DC motor can be written in terms of equations as follows [19:25]. These non linear model equations can be simulated with using Matlab/Simulink in overall system:

$$\frac{di_a(t)}{dt} = \frac{V_t(t)}{L_a + L_f} - \frac{R_a + R_f}{L_a + L_f} i_a(t) - \frac{M_{af}}{L_a + L_f} i_a(t) \omega_r(t) \quad (21)$$

$$\frac{d\omega_r(t)}{dt} = \frac{M_{af}}{J} i_a^2(t) - \frac{f}{J} \omega_r(t) - \frac{T_L}{J} \quad (22)$$

where

- i_a = The motor current,
- V_t = The motor terminal voltage,
- R_a, L_a = The armature resistance and inductance,
- R_f, L_f = The field resistance and inductance,
- ω_r = The motor angular speed,
- J = The moment of inertia,
- T_L = The load torque,

f = The friction coefficient,

M_{af} = The mutual inductance between the armature and field.

8.2. Digital Simulation Results of DC Series Motor

Using the values of the EFLSC parameters with the overall system for DC series motor Fig 7 shows step change of load torque at constant radiation and temperature for PV source. Figure 8 illustrated the motor output speed response to 2000 rpm for step change of maximum allowable load torque. To show the influence of load torque on speed, a load torque change from no load to 18.85 Nm (full load) is applied to the motor at time = 0.3sec then removed after 0.3 sec at time=0.6 sec. From speed response it is found the MPPT technique reduces the speed over shoot with load change. Figure 9 illustrated the step change load torque from no load – full load – no load at each step of speed change. This figure illustrates the variable radiation and temperature for PV system. But figure 10 illustrates the reference and actual speed for the motor with and without MPPT without speed controller. From this figure it is found that by using MPPT reduces the number of PV module.

Figure 11 illustrates the reference and actual speed for the motor with and without MPPT using the EFLSC controller. This figure shows that the actual speed reaches to steady state value after around 0.05 sec and no critically damped response. Also, minimum overshoot for speed response at each change of speed reference or load torque. This reason of this speed overshoot of the mechanical equation for series DC motor as Eqn. 22 is secondary order equation.

Figure 12 shows the instantaneous motor current with and without MPPT.

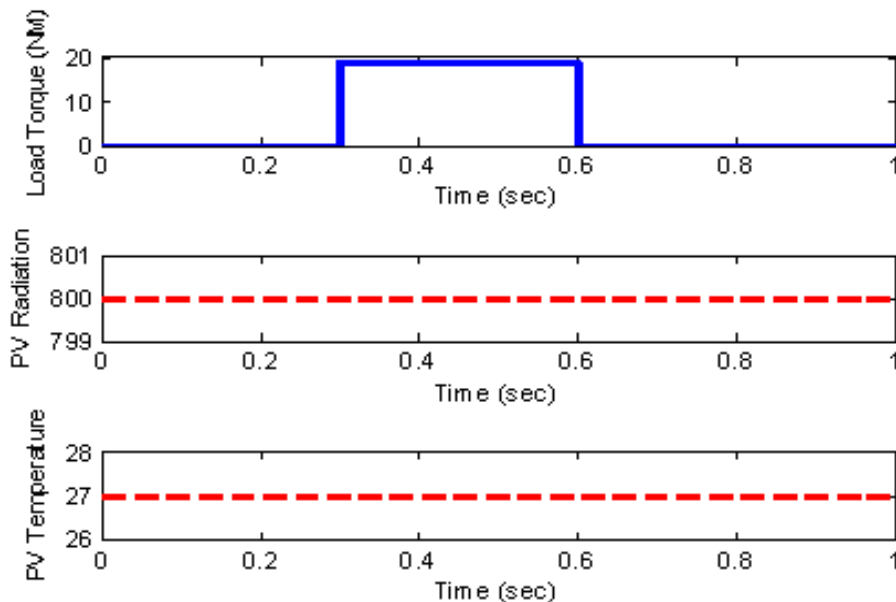


Fig. 7: The step change of load torque, with constant radiation and constant temperature for PV system.

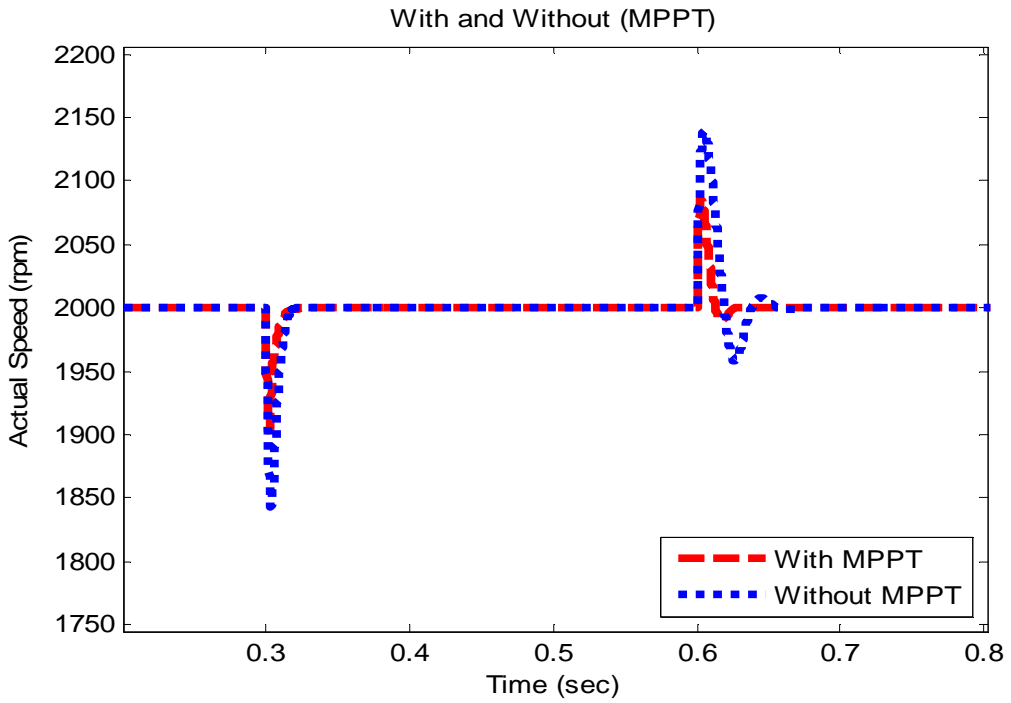


Fig. 8: The motor actual speed with and without MPPT under focusing.

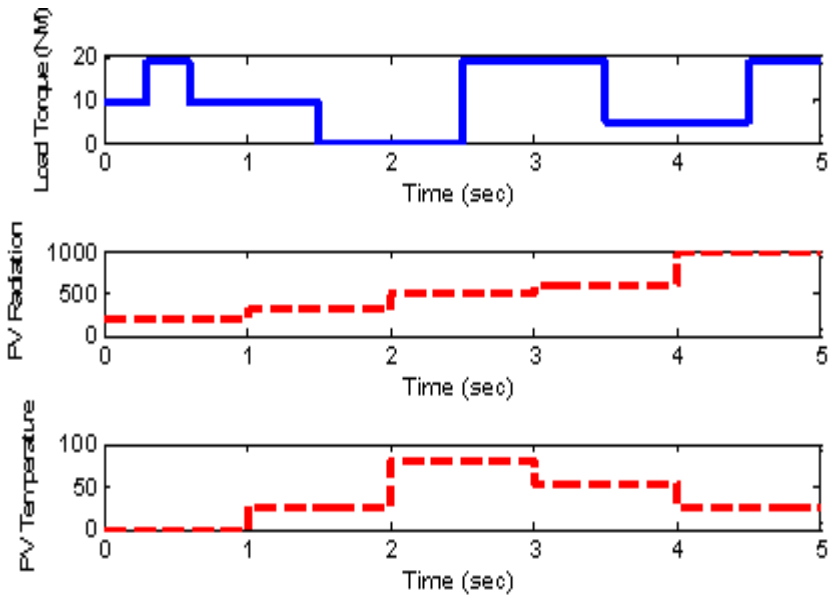


Fig. 9: The variable load torque, with variable radiation and variable temperature for PV system.

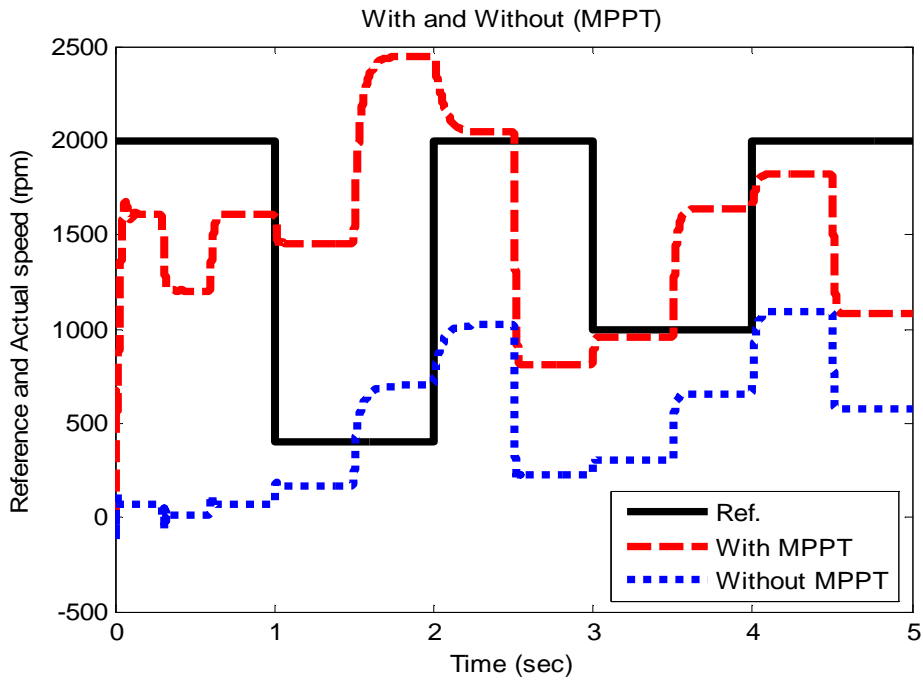


Fig. 10: The reference and actual speed with and without MPPT without using EFLSC controller.

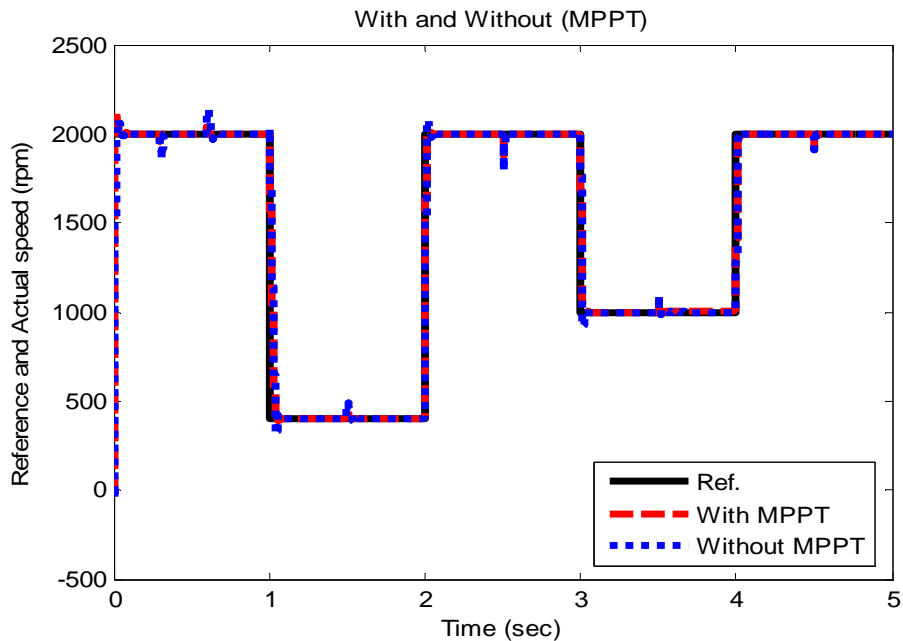


Fig. 11: The reference and actual speed with and without MPPT with using EFLSC controller.

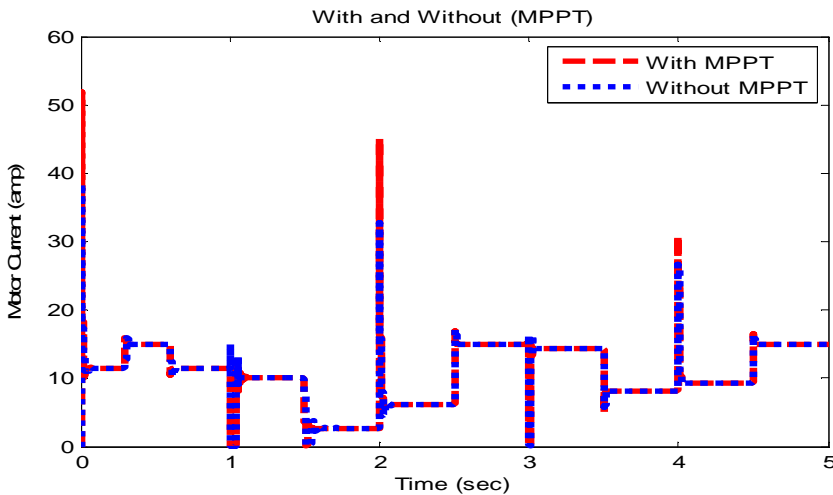


Fig. 12: The motor current with and without MPPT with using EFLSC controller.

9. DC PERMANENT MAGNET MOTOR

9.1. DC Permanent Magnet Motor Construction

The permanent magnet DC machines are widely found in a wide variety of low power applications. The field winding is replaced by a permanent magnet, resulting in simpler construction. Permanent magnets offer a number of useful benefits in these applications. The space required for the permanent magnets may be less than that required for the field winding and thus permanent- magnet machines may be smaller , and in some case cheaper , than their externally- excited counterparts.

Alternatively, permanent magnet DC machines are subjected to limitations imposed by the permanent magnets themselves. These include the risk of demagnetization due to excessive currents in the motor windings or due to overheating of the magnet. In addition, permanent magnets are somewhat limited in the magnitude of air gap flux density that they can produce. However, with the development of new magnetic materials such as samarium-cobalt and neodymium-iron-boron, these characteristics are becoming less restrictive for permanent-magnet machine design [24,25].

The proposed system can be simulated with proper mathematic modeling. The permanent magnet DC motor can be written in terms of equations as follows [3,4] and [16-23]. The non linear model equations can be simulated using Matlab/Simulink in overall system:

$$\frac{di_a(t)}{dt} = \frac{V_t(t)}{L_a} - \frac{R_a}{L_a}i_a(t) - \frac{K_v}{L_a}\omega_r(t) \quad (23)$$

$$\frac{d\omega_r(t)}{dt} = \frac{K_v}{J}i_a(t) - \frac{f}{J}\omega_r(t) - \frac{T_L}{J} \quad (24)$$

where ,

i_a = The motor current,

V_t = The motor terminal voltage,
 R_a, L_a = The armature resistance and inductance,
 ω_r = The motor angular speed,
 J = The moment of inertia,
 T_L = The load torque,
 f = The friction coefficient,
 K_v = The field constant.

9.2. Digital Simulation Results of DC Permanent Magnet Motor

Using the values of the EFLSC parameters with the overall system for permanent magnet DC motor Fig. 13 shows a step change of load torque at constant radiation and constant temperature for PV source. Figure 14 illustrates The motor actual speed with and without MPPT under focusing of DC Permanent Magnet Motor. To show the influence of load torque on speed, a load torque change from no load to 18.85 Nm full load is applied to the motor at time=0.3sec then removed after 0.3 sec at time=0.6 sec. Figure 15 depicts the step change for load torque from no load – full load – no load at each step of speed change and this figure illustrates the variable radiation and variable temperature for PV system. Figure 16 shows the reference and actual speed for the motor with and without MPPT without using EFLSC controller. From this figure it is found that by using MPPT, the number of PV module is reduced. Figure 17 illustrates the reference and actual speed for the motor with and without MPPT with using EFLSC controller. This figure shows that the actual speed arrive to steady state value after around 0.05 sec with critically damped response because. The reason for no speed overshoot is that the mechanical equation for permanent magnet DC motor (Eqn. 24) is first order equation. From figure 17 shows that the calculated EFLSC parameters can ensure a fast response is seen from figure and critically damped response for the motor output speed even with different maximum acceleration of the system. Figure 18 illustrated the instantaneous motor current with and without MPPT with EFLSC controller of DC permanent magnet motor.

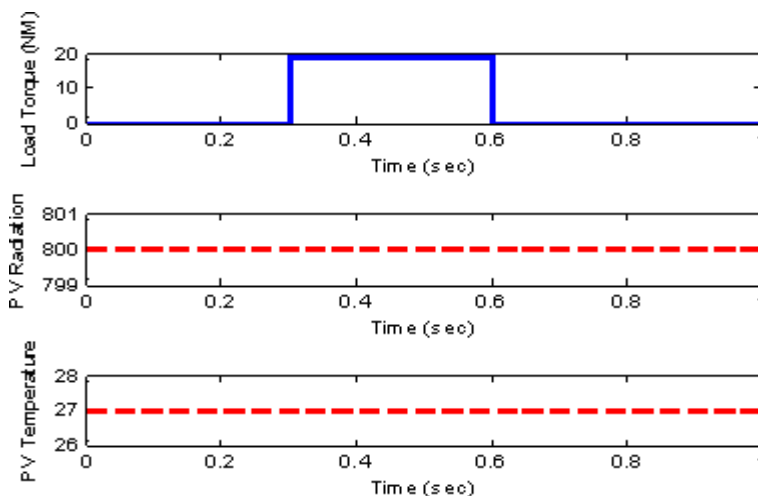


Fig. 13: The step change of load torque, with constant radiation and constant temperature for PV system of DC Permanent Magnet Motor.

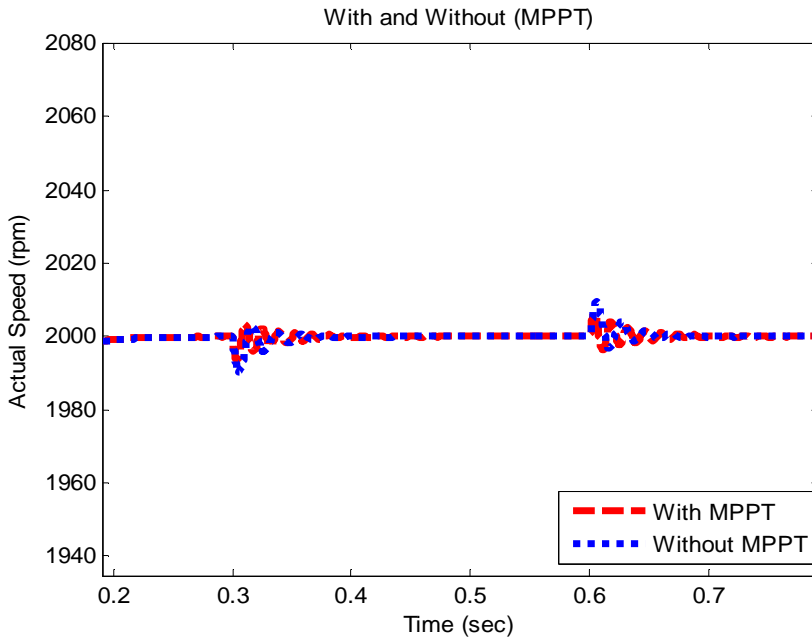


Fig. 14: The motor actual speed with and without MPPT for DC Permanent Magnet Motor.

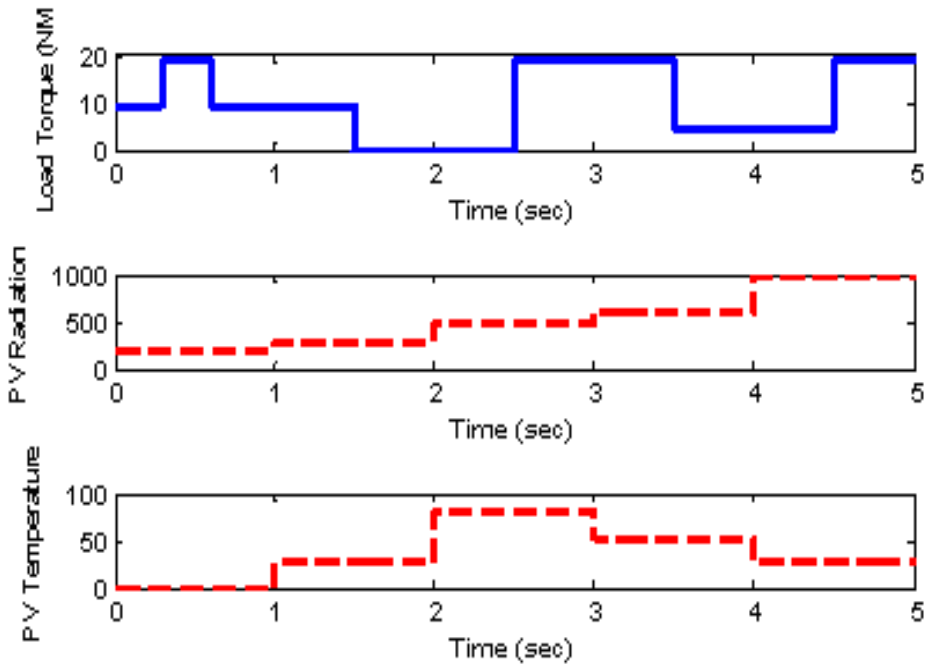


Fig. 15: The variable load torque, with variable radiation and variable temperature for PV system of DC Permanent Magnet Motor.

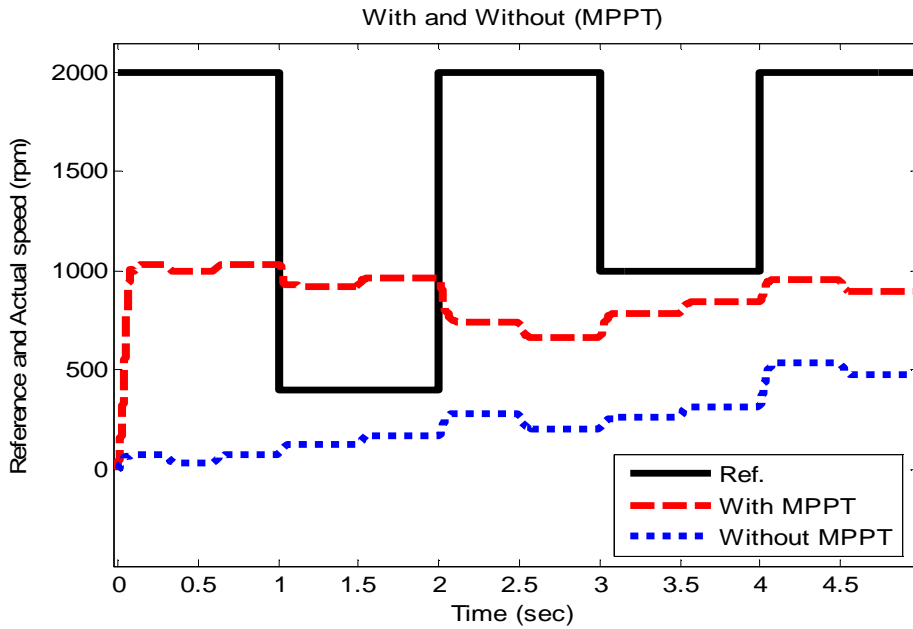


Fig. 16: The reference and actual speed with and without MPPT without using EFLSC controller for DC Permanent Magnet Motor.

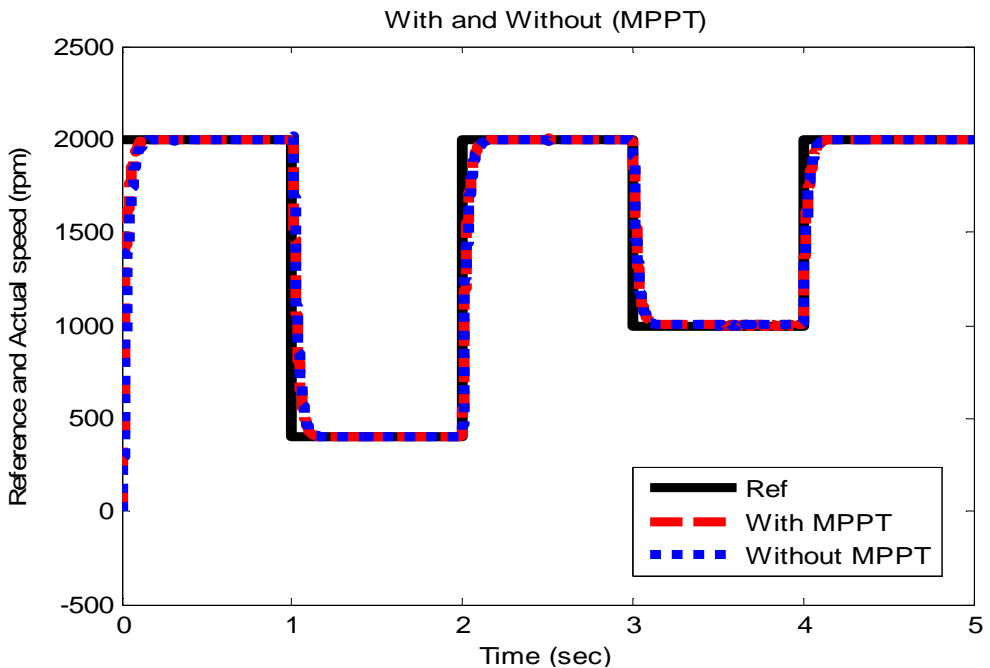


Fig. 17: The reference and actual speed with and without MPPT with using EFLSC controller for DC Permanent Magnet Motor.

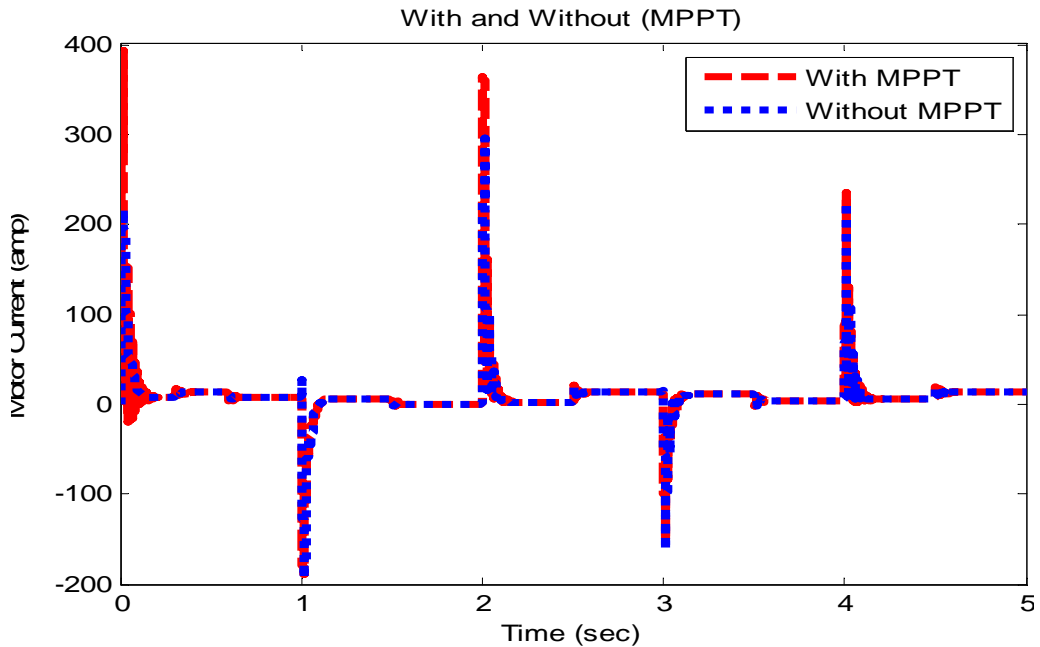


Fig. 18: The motor current with and without MPPT with EFLSC controller for DC Permanent Magnet Motor.

10 . CONCLUSIONS

This paper proposes a PID approach for controlling MPPT of a photovoltaic system. The conventional controller for MPPT was simulated using a buck-boost converter. The simulation results demonstrate that the controller is able to deal with system parameters and disturbances with good and fast transient performance under all conditions. Also this paper introduces an efficient fuzzy logic speed controller (EFLSC) for different types of DC motors supplied from PV system using MPPT technique. The EFLSC is the advantage of both the classical controllers and the intelligent controllers. The Fuzzy logic controller idea is used to obtain the EFLSC output equation, where the EFLSC equation is based on the speed error and its change of error. The EFLSC is simulated in s-domain using the MATLAB/SIMULINK program. The EFLSC parameters are calculated based on the motor mechanical equation and a predefined system performance. The EFLSC is applied to an accurate speed control technique for series DC motor model and also for permanent magnet DC motor model. The EFLSC is used to control the motor speed at variable load torque, variable radiation, and variable temperature for PV system. The input voltage for DC motor is changed by adjusting the duty ratio for DC/DC converter. buck-boost converter is used as a coupling between the PV system and DC motors. The speed responses for a variety of operating conditions are studied. Simulation results show that the EFLSC controller is active performance at all the operating conditions.

REFERENCES

- [1] Muhammad H.Rashid, "Power electronics circuits", devices and applications", 2d edition, Prentice-Hall, 1993.
- [2] Philip.T.Krein, "Elements of power Electronics", Oxford University Press, 1998.
- [3] N.Senthil Kumar, V.Sadasivam, K.Prema, "Design and simulation of fuzzy controller for closed loop control of chopper fed embedded dc drives", IEEE international conference, POWERCON, Singapore, 2004.
- [4] H.A.Yousef,H.M.Khalil "A fuzzy logic-based control of series DC motor drives", Proceedings of the IEEE International Symposium on Volume 2, Issue , 10-14 Jul1995 Page(s):517 – 522.
- [5] M. Veerachary, T. Seniyu and K. Uezato, "Maximum power point tracking control of IDB converter supplied PV system", IEE Proc. Electronic Power Applications, Vol. 148. No. 6, PP. 494 . 502, Nov. 2001.
- [6] S. Armstrong and W. Hurley, " Self – regulating maximum power point tracking for solar energy systems" Power Electronics Research Center, National University of Ireland , Galaway, PP. 604 . 609, 2001.
- [7] H. J. Moller, "Semiconductor for solar cells", Artech house Inc, Norwood, MA, 1993.
- [8] R. Gottschalg, M. Rommel, D. G. Ineld, & H. Ryssel, "Comparison of different methods for the parameter determination of the solar cells double exponential equation" 14th European Science & Engineering Conference (PVSEC), Barcelona, Spain, 1997.
- [9] C. F. Lu, C. C. Liu, & C. J. Wu, "Dynamic modeling of battery energy storage system and application to power system stability", IEE Proceedings Generation, Transmission & Distribution, Vol.142, No.4, pp.429-435, July, 1995.
- [10] K. Hussein, I Muta, T. Hoshino and M. Oskada, "Maximum photovoltaic Power Tracking; An algorithm for rapidly changing atmospheric conditions", IEEE Proceedings Generation, transmission and Distribution, Vol. 142, No 1, PP.59. 64, 1995.
- [11] B. K. Bose, "Power electronics on ac drives", Englewood Cliffs, New Jersey: Prentice-Hall, 1986.
- [12] B. K. Bose, "Microcomputer control of power electronics and drives", New York, IEEE Press 1987.
- [13] Fayez El-Sousy and M. M. Salem, "Robust neural network controllers for indirect field orientation control of induction machine drive system", Proceedings of the 2002 International Conference on Control and Application, Xiamen, China, pp.1263-1268, June 2002.
- [14] Ahmed Rubaai and M. Kankam, "Adaptive tracking controller for induction motor drives using on-line training of neural networks" IEEE Trans. Industrial Appl., vol. 36, no. 5, Sep./Oct. 2000.
- [15] Ahmed M. Kassem and Ali M. Yousef " Robust MPPT control design and dynamic performance of a PV-Generator powered DC-motor pump system" , 13th middle East Power System Conference IEEE , MEPCON' 2009, Assiut university, Egypt, 20-23 December 2009, pp. 379-384.
- [16] B. K. Bose, "Expert systems, fuzzy logic, and neural networks applications in power electronics and motion control ", Proc. IEEE, vol. 82, pp.1303-1323,

- Aug. 1994.
- [17] P. Vas, "Artificial-Intelligent based electric machines and drives", New York: Oxford Univ. Press, 1999.
- [18] B. K. Bose, "Modern power electronics and ac drives", New Jersey: Prentice-Hall, 2002.
- [19] H.L.Tan " A simplified fuzzy logic controller for DC series motor with Improve performance " IEEE International Conference on Fuzzy System. 2001 pages 1523-1526.
- [20] N. Senthil Kumar, V. Sadasivam, M. Muruganandam "A Low-cost Four-quadrant Chopper-fed Embedded DC Drive Using Fuzzy Controller", Inter National Journal of Electric Power Components and Systems, Volume 35, Issue 8 August 2007 , pages 907 – 920.
- [21] Kareem M.Khan, Roland Primer "Signal Tracking Fuzzy Logic Controller for DC-DC Converters" IEEE -1999 pages 306-309.
- [22] "MATLAB Math Library User's Guide", by the Math Works. Inc., 2010.
- [23] Rajani K. Mudi and Nikhil R. Pal, Member, "A Robust Self-Tuning Scheme for PI- and PD-Type Fuzzy Controllers" IEEE Transactions On Fuzzy Systems, VOL. 7, NO. 1, FEBRUARY 1999. Pages 2-16.
- [24] Jabri, Majed; Chouiref, Houda; Jerbi, Houssein; Benhadj Braiek, Naceur; "Fuzzy logic parameter estimation of an electrical system" Systems, Signals and Devices, 2008. IEEE SSD 2008. 5th International Multi-Conference on 20-22 July 2008 Page(s):1 - 6 Digital Object Identifier 10.1109/SSD.2008.4632881.
- [25] T.Gupta, R.Boudreax, R.M.Nelms and John Y Hung "Implementation of a Fuzzy Controller for DC-DC Converters Using an Inexpensive 8-Bit micro controller", IEEE Trans. on Industrial Electronics, vol.44, no.5, October, 1997, pp.661-667.

التحكم فى سرعة انواع مختلفة من مواتير التيارالمستمر التى تغذى بخلايا شمسية عند

اقصى قدرة بواسطة التحكم المبهم المنطقى الفعال

هذه المقالة تقدم طريقة التحكم المبهم المنطقى الفعال فى سرعة انواع مختلفة من مواتير التيار المستمر وهما (موتور التيار المستمر توصيل على التوالى و ايضا موتور التيار المستمر ذو المغناطيس الثابت)، هذه المواتير تغذى بواسطة خلايا شمسية عند اقصى قدرة عند طريق خط محول تيار مستمر بين الخلايا و المواتير، التحكم فى السرعة يوضح فكرة التحكم المنطقى فى صورته الكلاسيكية، و ايضا هذا التحكم يجمع بين مميزات التحكم الكلاسيك و التحكم المتطور المنطقى المبهم، ثوابت التحكم تعتمد على حسابات المعادلات الميكانيكية للمواتير و معرفة اداء السرعة ، المعادلات الميكانيكية لكلا الموتورين يمكن تمثيلهم فى معادلات تفاضلية من الدرجة الاولى و الثانية ، باستخدام التغير فى زمن الدورة للمقوم نستطيع ان نتحكم فى جهد التغذية للمواتير و بالتالى يمكن التحكم فى السرعة ، اداء كلا الموتورين عند تغيير الحمل و تغيير السرعة اخذ فى النتائج، التحكم المقترح بواسطة التحكم المنطقى المبهم الفعال يوضح افضلية فى الاداء ، و زيادة على ذلك تقدم المقالة التحكم المبني على PID للتحكم فى حساب اقصى قدرة للخلايا عند ظروف تشغيل مختلفة و احمال متغيرة.